Experimental Joint Quantum Measurements with Minimum Uncertainty

Martin Ringbauer,[1,2,*] Devon N. Biggerstaff,[1,2] Matthew A. Broome,[1,2] Alessandro Fedrizzi,[1,2] Cyril Branciard,[1] and Andrew G. White[1,2]

[1]*Centre for Engineered Quantum Systems, School of Mathematics and Physics, University of Queensland, Brisbane QLD 4072, Australia*

[2]*Centre for Quantum Computer and Communication Technology, School of Mathematics and Physics, University of Queensland, Brisbane QLD 4072, Australia*

(Received 27 August 2013; published 15 January 2014)

Quantum physics constrains the accuracy of joint measurements of incompatible observables. Here we test tight measurement-uncertainty relations using single photons. We implement two independent, idealized uncertainty-estimation methods, the three-state method and the weak-measurement method, and adapt them to realistic experimental conditions. Exceptional quantum state fidelities of up to 0.999 98(6) allow us to verge upon the fundamental limits of measurement uncertainty.

DOI: 10.1103/PhysRevLett.112.020401 PACS numbers: 03.65.Ta, 03.67.-a, 42.50.Ex, 42.50.Xa

Measurement—assigning a number to a property of a physical system—is the keystone of the natural sciences. Our belief in perfect measurement precision was shattered by the paradigm shift heralded by quantum physics almost a century ago. It is, perhaps, surprising that even today active debate persists over the fundamental limits on measurement imposed by quantum theory.

At the heart of this debate is Heisenberg's uncertainty principle [1], which encompasses at least three distinct statements about the limitations on preparation and measurement of physical systems [2]: (i) a system cannot be prepared such that a pair of noncommuting observables (e.g., position and momentum) are arbitrarily well defined; (ii) such a pair of observables cannot be jointly measured with arbitrary accuracy; and (iii) measuring one of these observables to a given accuracy disturbs the other accordingly.

The preparation uncertainty (i) was quantified rigorously by Kennard as [3]

$$\Delta x \Delta p \geq \hbar/2, \tag{1}$$

where Δx and Δp are the standard deviations of the position and momentum distributions of the prepared quantum system, respectively. For measurement uncertainty (ii) and (iii), the corresponding quantities of interest are the measurement inaccuracies ε and disturbances η. In his original paper [1], Heisenberg argued that the product of ε_x and η_p should obey a similar bound to (1) in a measurement-disturbance scenario; however, a formal proof was long lacking. Recently, Busch *et al.* provided such a proof for a relation of the form $\varepsilon_x \eta_p \geq \hbar/2$ [4].

However, there has been controversy on whether such a relation holds in full generality [4–10]. The point of contention is the choice of exact definitions for the measurement inaccuracies ε and disturbances η. In their derivation, Busch *et al.* [4] independently maximized the inaccuracies and disturbances over all possible quantum states for a given measurement apparatus; hence, their inaccuracies and disturbances are in general defined for different states. When both quantities are defined on the same quantum state, the relation $\varepsilon_x \eta_p \geq \hbar/2$ does not necessarily hold [5,6].

Following this observation, Ozawa [11,12] and Hall [13] derived new relations for the joint-measurement and the measurement-disturbance scenarios for any pair of observables. These were recently tested experimentally with neutronic and photonic qubits [14–18], demonstrating violation of a generalization of the above relation. Although universally valid, neither Ozawa's nor Hall's relations are optimal; Branciard improved these and derived tight relations quantifying the optimal trade-off between inaccuracies in approximate joint measurements and between inaccuracy and disturbance [19] for the definitions of ε and η used by Ozawa and Hall.

Here, we test Branciard's new relations by performing approximate joint measurements of incompatible polarization observables on single photons; see Fig. 1(a). We verify that we can get close to saturating these relations in practice. Although framed within the joint-measurement scenario, our analysis also applies to the measurement-disturbance scenario, illustrated in Fig. 1(b), in which case the inaccuracy ε_B can be interpreted as the disturbance η_B on B.

We use two independent methods for estimating inaccuracies and disturbances experimentally: the three-state method [20] and the weak-measurement method [21]. The three-state method requires the preparation of multiple input states. The weak-measurement method, in turn, more closely resembles the classical approach for measuring inaccuracies, but comes at the cost of a more challenging experiment. Crucially, both methods were defined under ideal conditions which are unattainable in practice. Therefore, we extend the respective estimation procedures to account for experimental imperfections—a step that has previously not received sufficient attention.

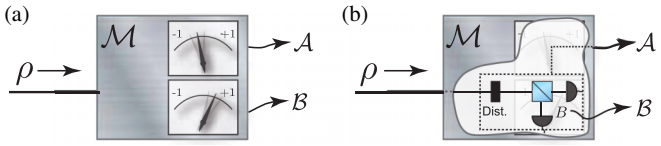

FIG. 1 (color online). (a) The approximate joint measurement scenario: a quantum state ρ is subjected to a measurement $\mathcal{M}$, from which observables $\mathcal{A}$ and $\mathcal{B}$ are extracted to approximate two incompatible observables A and B, respectively. (b) In our implementation, an actual measurement of B is performed after ρ is disturbed (to also obtain an approximation of A). By opening the black box $\mathcal{M}$, our experiment can also be interpreted—when $\mathcal{B}$ is directly extracted from the disturbed measurement of B—as implementing the measurement-disturbance scenario. Note that this scenario requires B and $\mathcal{B}$ to have the same spectrum.

Theoretical framework.—Let ρ denote a quantum state, and let A and B be two observables. The (in)compatibility of A and B when measured on ρ is quantified by the parameter $C_{AB} = \frac{1}{2i}\mathrm{Tr}[(AB - BA)\rho]$: whenever $C_{AB} \neq 0$, they do not commute and cannot be jointly measured on ρ. However, one may still approximate their joint measurement using an observable $\mathcal{M}$ [or, more generally, a positive operator-valued measure (POVM) $\mathbb{M}$ [22]] and defining approximations $\mathcal{A} = f(\mathcal{M})$ and $\mathcal{B} = g(\mathcal{M})$ [23], see Fig. 1. Specifically, for an outcome m of $\mathcal{M}$ and real-valued functions f and g, one outputs $f(m)$ to approximate the measurement of A, and $g(m)$ to approximate the measurement of B. Following Ozawa [11,12], one can quantify the inaccuracies of these approximations by the root-mean-square errors

$$\varepsilon_{\mathcal{A}} = \mathrm{Tr}[(\mathcal{A} - A)^2\rho]^{1/2}, \qquad \varepsilon_{\mathcal{B}} = \mathrm{Tr}[(\mathcal{B} - B)^2\rho]^{1/2}. \quad (2)$$

Branciard showed in [19] that, for any approximate joint measurement, the above definitions of $\varepsilon_{\mathcal{A}}$ and $\varepsilon_{\mathcal{B}}$ satisfy the uncertainty relation for approximate joint measurements

$$\Delta B^2\varepsilon_A^2 + \Delta A^2\varepsilon_B^2 + 2\sqrt{\Delta A^2\Delta B^2 - C_{AB}^2}\varepsilon_A\varepsilon_B \geq C_{AB}^2, \quad (3a)$$

where $\Delta A = (\mathrm{Tr}[A^2\rho] - \mathrm{Tr}[A\rho]^2)^{1/2}$ and $\Delta B = (\mathrm{Tr}[B^2\rho] - \mathrm{Tr}[B\rho]^2)^{1/2}$ are the standard deviations of A and B on the state ρ. Furthermore, when ρ is pure, this relation is tight [19]: it quantifies the optimal trade-off in the inaccuracies of the approximate measurements $\mathcal{A}$ and $\mathcal{B}$.

Interestingly, saturating Eq. (3a) may require the approximate observables $\mathcal{A}$ and $\mathcal{B}$ to have different spectra from A and B—i.e., the optimal output values $f(m)$ and $g(m)$ may not be eigenvalues of A and B. One may, nevertheless, want to impose that the approximations $\mathcal{A}$ and/or $\mathcal{B}$ have the same spectrum as A and B: this assumption is natural for $\mathcal{B}$ in a measurement-disturbance scenario, where $\mathcal{B}$ corresponds to an actual measurement of B after ρ is disturbed; see Fig. 1(b). With this restrictive same-spectrum assumption, one can, in general, derive stronger relations than (3a) [19]. For instance, in the case of ± 1-valued observables (such that $A^2 = B^2 = \mathbb{1}$), when also imposing $\mathcal{A}^2 = A^2 = \mathbb{1}$ and/or $\mathcal{B}^2 = B^2 = \mathbb{1}$, relation (3a) can be strengthened as follows [19,24]: Eq. (3a) with replacements

$$\varepsilon_{\mathcal{A}} \to \sqrt{1 - (1 - \varepsilon_{\mathcal{A}}^2/2)^2}, \qquad \varepsilon_{\mathcal{B}} \to \sqrt{1 - (1 - \varepsilon_{\mathcal{B}}^2/2)^2}, \quad (3b)$$

where the replacement is made for the observable(s) on which the same-spectrum assumption is imposed.In order to test the relations (3a) and (3b) experimentally, one must determine the inaccuracies $\varepsilon_{\mathcal{A}}$ and $\varepsilon_{\mathcal{B}}$. If we expand Eq. 2 (see the Supplemental Material [25]), $\varepsilon_{\mathcal{A}}$ can be related to the measurement statistics of $\mathcal{M}$ in the states ρ, $A\rho A$ and $(\mathbb{1} + A)\rho(\mathbb{1} + A)/\|\cdot\|$, motivating the three-state method [20]. Alternatively, the weak-measurement method [21] links the definition of $\varepsilon_{\mathcal{A}}$ to the joint probability distribution of an initial weak measurement of A, followed by a measurement of $\mathcal{M}$. These two independent techniques allow us to estimate $\varepsilon_{\mathcal{A}}$ and $\varepsilon_{\mathcal{B}}$ without any assumptions about the actual measurement apparatus.

Experimental implementation.—Our experimental demonstration was performed with polarization-encoded qubits; see Fig. 2. Denoting the Pauli matrices $\sigma_{x,y,z}$, and their eigenstates $|\pm x, y, z\rangle$, we prepared $\rho = |+y\rangle\langle+y| = (\mathbb{1} + \sigma_y)/2$ in the case of the three-state method, and $\rho = (\mathbb{1} + \sqrt{1-\kappa^2}\sigma_y)/2$ for the weak-measurement method, where $\kappa \in [-1, 1]$ quantifies the measurement strength. On these states we approximated the joint measurement of the incompatible observables $A = \sigma_x$ and $B = \sigma_z$. For ideal states ρ, one finds $C_{AB}^2 = 1$ and $C_{AB}^2 = 1 - \kappa^2$, respectively.

The measurement apparatus implementing the joint approximation of A and B was chosen to perform a projective measurement $\mathcal{M} = \cos\theta\sigma_z + \sin\theta\sigma_x$ onto a direction in the xz plane of the Bloch sphere. In our experiment, this was realized by a half-wave plate and a polarizing prism which projected onto $|-z\rangle$, Fig. 2. The outcomes $m = \pm 1$ of the measurement of $\mathcal{M}$ were then used to output some values $f(m)$ and $g(m)$. These values were either chosen to minimize the inaccuracies $\varepsilon_{\mathcal{A}}$ and $\varepsilon_{\mathcal{B}}$, or set to ± 1 in the case where the same-spectrum assumption was imposed [25].

For both experiments data were acquired for a series of settings $\theta \in [0, 2\pi]$ of $\mathcal{M}$. We emphasize that in the calculations of $\varepsilon_{\mathcal{A}}$ and $\varepsilon_{\mathcal{B}}$ from either technique, we used neither the angle θ nor did we make any assumptions on the internal functioning of the measurement apparatus (e.g., that it implements a projective measurement): it is considered a black box that performs a fully general POVM with classical outputs $m = \pm 1$.

The three-state method.—For this method [20], in addition to the state $\rho \simeq |+y\rangle\langle+y|$, we prepared the states $\rho_1 \simeq A\rho A \simeq B\rho B \simeq |-y\rangle\langle-y|$ and $\rho_2 \simeq (\mathbb{1}+A)\rho(\mathbb{1}+A)/\|\cdot\| \simeq |+x\rangle\langle+x|$ [respectively, $\rho_2' \simeq (\mathbb{1}+B)\rho(\mathbb{1}+B)/\|\cdot\| \simeq |+z\rangle\langle+z|$], and characterized them using overcomplete quantum state tomography [27]. The values of

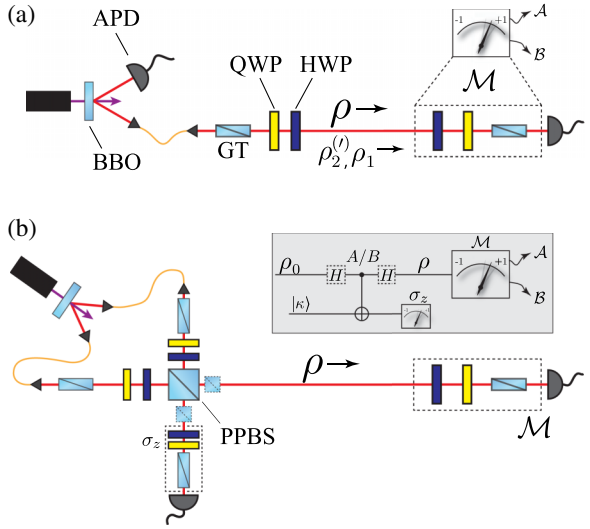

FIG. 2 (color online). Experimental setup. (a) Three-state method. Single photons at a wavelength of $\lambda = 820$ nm were produced in a noncollinear type-I spontaneous parametric down-conversion (SPDC) source using a β-barium-borate (BBO) nonlinear crystal, pumped by a frequency-doubled fs-pulsed Ti:sapphire laser. State preparation was performed by Glan-Taylor polarizers (GT), a quarter-wave plate (QWP), and a half-wave plate (HWP). A HWP at an angle of $(\theta/4)$ and a polarizer implemented the measurement $\mathcal{M}$. The additional QWP between these elements was used for state tomography, with avalanche photodiodes (APD) used for detection. (b) Weak-measurement method. State preparation and final measurement were realized as in (a). The weak measurement relied on a controlled-phase gate based on two-photon interference at a partially polarizing beam splitter (PPBS) with nominal reflectivities of $R_H = 0$ and $R_V = 2/3$ for horizontal and vertical polarization, respectively [26]. The required amplitude compensation (dashed PPBS) was performed via prebiased input states and all Hadamard gates were incorporated into either the state-preparation or the measurement wave plates. The corresponding circuit diagram is shown in the gray inset. Note that the controlled-NOT gate is equivalent to a controlled-phase gate between Hadamard gates in the meter arm.

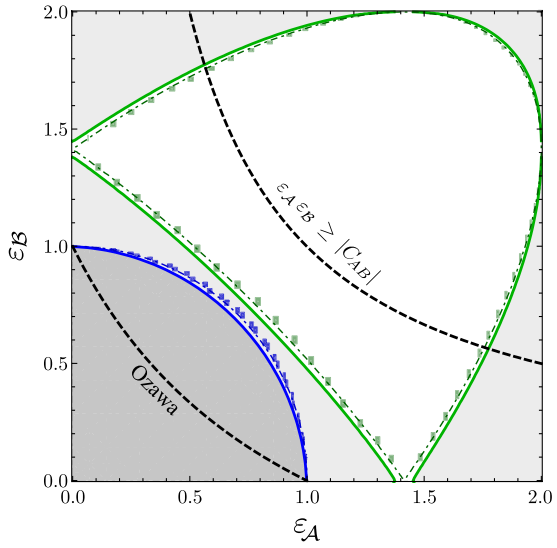

FIG. 3 (color online). Experimental measurement inaccuracies, $\varepsilon_{\mathcal{A}}$ vs $\varepsilon_{\mathcal{B}}$, characterized by the three-state method. The blue rectangles represent the intervals of compatible values of $\varepsilon_{\mathcal{A}}$ and $\varepsilon_{\mathcal{B}}$ without the same-spectrum assumption. The solid blue curve corresponds to the bound imposed by the relation (3a), for the experimental values of ΔA, ΔB, and C_{AB}; the values below this bound are forbidden by quantum theory. The dotted-dashed blue line is the bound imposed by (3a) for the ideal case $\Delta A = \Delta B = C_{AB} = 1$. The green rectangles and curves represent the corresponding data when the same-spectrum assumption is imposed on both $\mathcal{A}$ and $\mathcal{B}$, now invoking relation (3b); note that in contrast to (3a), this relation also upper bounds the values of $\varepsilon_{\mathcal{A}}$ and $\varepsilon_{\mathcal{B}}$. For comparison, the black dashed curves indicate the bounds imposed by the relation $\varepsilon_{\mathcal{A}}\varepsilon_{\mathcal{B}} \geq |C_{AB}|$—which is violated by our data—and by Ozawa's relation [11,12]—which is indeed satisfied, but cannot be saturated. Note that the shown intervals include 1σ statistical errors obtained from Monte Carlo sampling assuming Poissonian photon-counting statistics.

$\varepsilon_{\mathcal{A}}$ (respectively, $\varepsilon_{\mathcal{B}}$) can then be estimated from the measurement statistics of $\mathcal{M}$ in these states [20,25].

The experimental setup is shown in Fig. 2(a). The initial state ρ was prepared on a heralded single photon with high quantum state fidelity $\mathcal{F} = 0.999\,172(7)$ and purity $\mathcal{P} = 0.999\,17(2)$, and gave $C_{AB}^2 = 0.996\,69(3)$. The states ρ_1 and ρ_2 were prepared with similar quality [25]. Figure 3 shows the results obtained for $\varepsilon_{\mathcal{A}}$ and $\varepsilon_{\mathcal{B}}$, without and with the same-spectrum assumption (imposed in the latter case on both $\mathcal{A}$ and $\mathcal{B}$; see [25] for the case where it is only imposed on $\mathcal{B}$). We get very close to saturating relations (3a) and (3b).

Importantly, the equations used for obtaining $\varepsilon_{\mathcal{A}}$ and $\varepsilon_{\mathcal{B}}$ in the original three-state proposal [20] assume perfect state preparation. Directly applying them to imperfect experimental states invalidates the derivation and leads to unreliable results. In the Supplemental Material [25], we extend the estimation procedure to realistic conditions. With careful characterization of the input states, our method yields finite intervals for $\varepsilon_{\mathcal{A}}$ and $\varepsilon_{\mathcal{B}}$ that are compatible with the experimental data, shown as shaded rectangles in Fig. 3.

The weak measurement method.—A weak measurement [28] aims at extracting partial information from a quantum system without disturbing it. It is typically realized by weakly coupling the system to a meter which is then subjected to a projective measurement. In practice, weak measurements cannot be infinitely weak—they disturb the state onto which they are applied. In our case, the joint measurement of A and B is then approximated on the disturbed state ρ after the (semi)weak measurement of A and B, respectively. Note that this disturbance necessarily introduces mixture to ρ. As a consequence, it may no longer be possible to saturate (3a) and (3b); in particular, C_{AB}^2 will be decreased. As noted in [16], the weak-measurement method actually works for any measurement strength. However, to approach saturation, one should set it as low as possible.

The experimental weak-measurement setup is shown in Fig. 2(b). We realized the weak measurement using a nondeterministic linear-optical controlled-NOT (CNOT) gate [26] acting on our initial signal qubit $\rho_0 = |+y\rangle\langle+y| = (\mathbb{1} + \sigma_y)/2$ and a meter qubit in the state $|\kappa\rangle = \sqrt{(1+\kappa)/2}|0\rangle + \sqrt{(1-\kappa)/2}|1\rangle$, which determines the measurement strength κ [28]. The CNOT gate alone, followed by a measurement of the meter qubit in the computational basis, enables the weak measurement of $B = \sigma_z$, while the weak measurement of $A = \sigma_x$ requires two additional Hadamard gates; see Fig. 2(b). In both cases, the initial state ρ_0 of the signal qubit is transformed to $\rho = (\mathbb{1} + \sqrt{1-\kappa^2}\sigma_y)/2$. In practice, the disturbed states ρ^A and ρ^B after the weak measurements of A and B, respectively, necessarily differ slightly. To account for that, we simply defined ρ—which enters the definitions of ΔA, ΔB, ε_A, ε_B, and C_{AB} in relations (3a) and (3b)—to be the averaged disturbed state $\rho = \frac{1}{2}(\rho^A + \rho^B)$.

We characterized the quality of our gate operation using quantum process tomography [29], obtaining a process fidelity of $\mathcal{F}_p = 0.964(1)$. We further measured a state fidelity of $\mathcal{F} = 0.999\,98(6)$ of the average disturbed state ρ, with a reduced purity of $\mathcal{P} = 0.964(1)$, corresponding to an average value of $\kappa = -0.262(4)$, for which we obtain $C_{AB}^2 = 0.928(2)$. For the two-qubit states ρ_{12}^A and ρ_{12}^B after the interaction (corresponding to the weak measurements of A and B, respectively), we find fidelities of $\mathcal{F} = 0.993\,8(6)$ and $\mathcal{F} = 0.995\,8(3)$. More details on the quality of the prepared states, the used measurement apparatus, and a full error analysis can be found in [25].

The derivations in the original proposal [21] for this method require the weak measurements to be perfect. As for the three-state method, we extend the estimation procedure for ε_A and ε_B to account for realistic experimental implementations and obtain intervals of compatible values, which are shown as rectangles which include 1σ statistical errors in Fig. 4. Furthermore, we find that, if we, instead of treating them separately, take into account experimental data from both weak measurements of A and B, the size of these intervals can be significantly reduced. The corresponding smaller intervals, shown as dark rectangles in Fig. 4, are now dominated by statistical errors; see [25] for details.

Discussion.—Our results agree with the theoretical predictions in all cases under consideration, indicating that one can indeed come close to saturating the measurement uncertainty relations (3a) and (3b) in the experiment. Unsurprisingly, the ranges of compatible values determined for the weak-measurement method are significantly larger than those for the three-state method. This is due to the experimentally more demanding two-photon interaction. Although we took great care in the preparation of the initial states as well as in the alignment of the optical setup, residual errors from imperfect optical components, nonoptimal spatiotemporal mode overlap, and Poissonian counting statistics decrease the quality of the final data. Note also that SPDC is not a true photon-pair source. While the three-state method is not sensitive to higher-order emissions, the detrimental effect on the weak measurement method has been limited by keeping the pump power at a very low level, resulting in an estimated multipair contribution of 0.000 24.

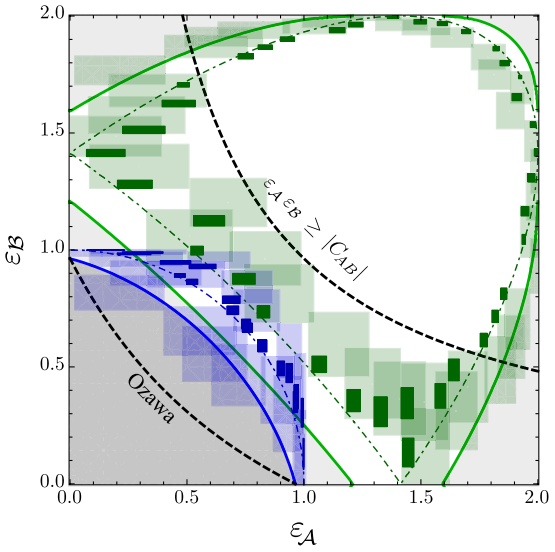

FIG. 4 (color online). Results obtained via the weak-measurement method, presented as in Fig. 3. The darker rectangles represent smaller intervals of compatible values obtained by using experimental data from both the weak measurements of A and B. All intervals include 1σ statistical errors.

To put our data into context with previously proposed measurement-uncertainty relations, Figs. 3 and 4 also show the relation $\varepsilon_A\varepsilon_B \geq |C_{AB}|$ [30,31] and Ozawa's relation [11,12]. While the latter is universally valid and indeed satisfied by our data (but not saturated, as it is not tight), the former relation only holds under some restrictive assumptions [6,30,31] for our definitions of ε_A, ε_B, and is clearly violated by our data.

Testing the ultimate measurement-uncertainty limits is crucial for our understanding of quantum measurements. The new relations introduced in [19] for both the joint measurement and the measurement-disturbance scenarios, and our comprehensive extension to experimental implementations, could play a role in refining a wide range of measurement-based quantum information protocols, such as quantum control or error correction. In particular, as detailed in [25], the optimal choice of approximating functions $f(m)$ and $g(m)$ in a joint-measurement experiment may differ from the theoretical optimum in the presence of experimental imperfections. Our technique of optimizing these quantities to find the optimal trade-off between ε_A and ε_B could be used as a calibration step in high-precision weak-, or joint-measurement experiments.

We thank G. G. Gillett and M. P. Almeida for assistance with the experiment. This work was supported in part by the Centres for Engineered Quantum Systems (CE110001013)

and for Quantum Computation and Communication Technology (CE110001027). A. F., C. B., and A. G. W. acknowledge support through Australian Research Council Discovery Early Career Award No. DE130100240, a University of Queensland (UQ) Postdoctoral Research Fellowship, and a UQ Vice-Chancellor's Senior Research Fellowship, respectively.

Note added.—Recently, we became aware of a related work by F. Kaneda *et al.* [32].

*m.ringbauer@uq.edu.au

[1] W. Heisenberg, Z. Phys. **43**, 172 (1927); J. A. Wheeler and W. H. Zurek, *Quantum Theory and Measurement* (Princeton University Press, Princeton, N.J., 1983), pp. 62–84.
[2] P. Busch, T. Heinonen, and P. Lahti, Phys. Rep. **452**, 155 (2007).
[3] E. Kennard, Z. Phys. **44**, 326 (1927).
[4] P. Busch, P. Lahti, and R. F. Werner, Phys. Rev. Lett. **111**, 160405 (2013).
[5] L. E. Ballentine, Rev. Mod. Phys.**42** 358 (1970).
[6] M. Ozawa, Phys. Lett. A **318**, 21 (2003).
[7] L. A. Rozema, D. H. Mahler, A. Hayat, and A. M. Steinberg, arXiv:1307.3604.
[8] M. Ozawa, arXiv:1308.3540.
[9] J. Dressel and F. Nori, arXiv:1308.4853.
[10] A. Di Lorenzo, Phys. Rev. Lett. **110**, 120403 (2013).
[11] M. Ozawa, Phys. Rev. A **67**, 042105 (2003).
[12] M. Ozawa, Phys. Lett. A **320**, 367 (2004).
[13] M. J. W. Hall, Phys. Rev. A **69**, 052113 (2004).
[14] J. Erhart, S. Sponar, G. Sulyok, G. Badurek, M. Ozawa, and Y. Hasegawa, Nat. Phys. **8**, 185 (2012).
[15] L. A. Rozema, A. Darabi, D. H. Mahler, A. Hayat, Y. Soudagar, and A. M. Steinberg, Phys. Rev. Lett. **109**, 100404 (2012).
[16] M. M. Weston, M. J. W. Hall, M. S. Palsson, H. M. Wiseman, and G. J. Pryde, Phys. Rev. Lett. **110**, 220402 (2013).
[17] G. Sulyok, S. Sponar, J. Erhart, G. Badurek, M. Ozawa, and Y. Hasegawa, Phys. Rev. A **88**, 022110 (2013).
[18] S.-Y. Baek, F. Kaneda, M. Ozawa, and K. Edamatsu, Sci. Rep. **3**, 2221 (2013).
[19] C. Branciard, Proc. Natl. Acad. Sci. U.S.A. **110**, 6742 (2013).
[20] M. Ozawa, Ann. Phys. (N. Y.) **311**, 350 (2004).
[21] A. Lund and H. M. Wiseman, New J. Phys. **12**, 093011 (2010).
[22] In general, the observable $\mathcal{M}$ can be replaced by POVM $\mathbb{M}$, as rigorously considered in [25]. Equivalently, $\mathcal{M}$ can be defined on a larger Hilbert space via a Neumark extension. The approximations of A and B are still defined by the functions $f(m)$ and $g(m)$, for the outcomes m of $\mathbb{M}$, and the definitions of $\varepsilon_{\mathcal{A}}$ and $\varepsilon_{\mathcal{B}}$ in Eq. (2) are easily generalized [25].
[23] Denoting by $|m\rangle$ the normalized eigenvector of $\mathcal{M}$ corresponding to the eigenvalue m, the approximate observables $\mathcal{A}$ and $\mathcal{B}$ are, thus, given by $\mathcal{A} = \sum f(m)|m\rangle\langle m|$ and $\mathcal{B} = \sum g(m)|m\rangle\langle m|$.
[24] C. Branciard, arXiv:1312.1857.
[25] See Supplemental Material at http://link.aps.org/supplemental/10.1103/PhysRevLett.112.020401 for details on the calculation of the inaccuracies $\varepsilon_{\mathcal{A}}$ and $\varepsilon_{\mathcal{B}}$, and on the characterization of our experiment.
[26] N. K. Langford, T. J. Weinhold, R. Prevedel, K. J. Resch, A. Gilchrist, J. L. O'Brien, G. J. Pryde, and A. G. White, Phys. Rev. Lett. **95**, 210504 (2005).
[27] D. F. V. James, P. G. Kwiat, W. J. Munro, and A. G. White, Phys. Rev. A **64**, 052312 (2001).
[28] G. J. Pryde, J. L. O'Brien, A. G. White, T. C. Ralph, and H. M. Wiseman, Phys. Rev. Lett. **94**, 220405 (2005).
[29] J. L. O'Brien, G. J. Pryde, A. Gilchrist, D. F. V. James, N. K. Langford, T. C. Ralph, and A. G. White, Phys. Rev. Lett. **93**, 080502 (2004).
[30] E. Arthurs and J. Kelly, Jr, Bell Syst. Tech. J. **44**, 725 (1965).
[31] E. Arthurs and M. S. Goodman, Phys. Rev. Lett. **60**, 2447 (1988).
[32] F. Kaneda, S.-Y. Baek, M. Ozawa, and K. Edamatsu, following Letter, Phys. Rev. Lett. **112**, 020402 (2014).